Pergamon

Int. J. Solids Structures Vol. 35, No. 33, pp. 4391–4410, 1998

0020–7683/98 $19.00 + .00

PII: S0020–7683(97)00214–X

THE CAVITY OF THE OPTIMAL SHAPE UNDER THE SHEAR STRESSES

A. V. CHERKAEV and Y. GRABOVSKY
Departments of Mathematics, University of Utah, Salt Lake City, UT 84112, U.S.A.

A. B. MOVCHAN and S. K. SERKOV†

School of Mathematical Sciences, University of Bath, Bath BA2 7AY, U.K.

(*Received* 22 *October* 1996; *in revised form* 22 *July* 1997)

Abstract—The problem of optimal shape of a single cavity in an infinite 2-D elastic domain is analyzed. An elastic plane is subjected to a uniform load at infinity. The cavity of the fixed area is said to be optimal if it provides the minimal energy change between the homogeneous plane and the plane with the cavity. We show that for the case of shear loading the contour of the optimal cavity is not smooth but is shaped as a curved quadrilateral. The shape is specified in terms of conformal mapping coefficients, and explicit analytical representations for components of the dipole tensor associated with the cavity are employed. We also find the exact values of angles at the corners of the optimal contour. The applications include the problems of optimal design for dilute composites. © 1998 Elsevier Science Ltd. All rights reserved.

1. INTRODUCTION

1.1. *The problem of shape optimization*

We consider the problem of maximization of the stiffness of an elastic plane weakened by a cavity of the fixed area and loaded by a uniform stress field $\boldsymbol{\sigma}$ at infinity. This problem is equivalent to minimizing the energy decrease stored in the medium. The total elastic energy stored in the plane is infinite, nevertheless, the energy decrease is finite. We constrain the cavity to occupy a simply-connected domain.

One would, perhaps, regard the problem of the optimal shape of a single cavity in an infinite plane to be a classical one. Indeed, it is known that the "best" cavity in a hydrostatic stress has a circular shape, and that the "best" cavities in the stress field which has eigenvalues of the same sign are ellipses. However, when the tensor, prescribed at infinity, has the eigenvalues of different sign, the shape of cavity (of fixed area) minimizing the energy increment seems to be unknown; it is appropriate to refer to the numerical experiments that have been carried out by Cherkaev and Vigdergauz (1986), where some characteristic features of the optimal shape were discussed.

The problem on optimal shape of solids has been initiated by Prager (1968) who has derived sufficient conditions of optimality. The shape of optimal cavities and the optimal properties of composites have been studied for a uniform hydrostatic loading and a biaxial loading with the principal stresses of the same sign (see Cherepanov, 1974; Vigdergauz, 1976; Vigdergauz, 1989). The optimal shapes of several cavities have been described by Vigdergauz (1988).

It is impossible to list in this short paper numerous publications dealing with structural optimization and, in particular, shape optimization. We would like to mention the monographs of Sokolowski and Zolesio (1992), Haug *et al.* (1986), Pironneau (1984) and Bendsoe (1995), and the review paper of Rozvany *et al.* (1994), that include mathematical and numerical analyses of shape sensitivity associated with elliptic boundary value problems. The existence of a solution of an optimal control formulation for boundary value problems for the Laplacian was analyzed by Chenais (1975). We are not aware of the analogous general result for the Lamé system. We refer the reader to the recent volume of Olhoff and

† Author to whom correspondence should be addressed.

Rozvany (1995) where the state of the art in structural optimization is fairly presented. Structural optimization through the FEM was discussed by Schnack *et al.* (1986).

In this paper, the main attention is paid to the case of pure shear loading. We show that the optimal cavity is a curved quadrilateral, and the angle near the corners is equal to the critical Carothers (1912) value $\sim 102.6^\circ$.

We start with the formulation of the optimization problem. Then we discuss the necessary conditions of optimality and applications to models of dilute composites. Next we present a minimization algorithm based on the concept of the dipole matrix corresponding to the remote field associated with finite cavities in an elastic plane. It enables one to produce explicit representation of the energy increment via the dipole coefficients. We represent the exterior of a cavity as a conformal image of the interior of the unit disc. Then we express the dipole matrix entries through the coefficients of the truncated Taylor expansion of that conformal map. Finally, we minimize the energy increment (given by the dipole tensor) over all possible values of the coefficients of the Taylor expansion. The resulting sequence of cavities exhibited a numerical convergence to a limiting shape of a quadrilateral described above.

Next we apply the complex variable technique closely following the method of Cherepanov (1974). We use optimality conditions and Kolosov–Muskhelishvili potentials in conjunction with conformal mapping representation of the unknown domain in order to set up the integral equation for the unknown conformal mapping. We reduce it to a finite dimensional system of linear equations by expanding everything into truncated power series. Solving the linear system, we recover the same numbers obtained by the direct minimization procedure described above.

Finally, we study the local behaviour of elastic fields near the corners of the cavity contour using the asymptotic expansion of the solution near the corner and the optimality conditions; in this way we find the exact value of the angle at the corner. The algorithms employed in this work can be effectively applied for any uniform load.

1.2. *Link with composite materials*

If one removes any restriction on the topology of the structure (number of holes) then one is led to consider composites—limiting materials with an infinite number of infinitely small holes (Kohn and Strang, 1986). The optimization problem for composites turned out to be easier to solve analyticaly (see, for example, the papers by Gibiansky and Cherkaev, 1984; Gibiansky and Cherkaev, 1986; Kohn and Strang, 1986; Milton, 1986; Bendsoe, 1995; Grabovsky and Kohn, 1995; the recent review paper by Rozvany *et al.*, 1994 has a number of additional references). These analytical solutions showed that in our setting the elliptical hole is a minimizer (one of the many) of the energy increment if the principal stresses have the same sign, even when the topology is unrestricted. However, if the principal stresses have opposite sign then a genuine composite, such as a second rank laminate, must be a minimizer. The "optimal" shape that we have found in our paper has a significantly higher energy increment than the optimal composite. Yet, our shape is the best if one restricts the number of holes to one.

2. PROBLEM FORMULATION

In this section we present the boundary value problem, give the appropriate variational formulation and discuss the optimality criteria.

2.1. *Elasticity problem*

First, we consider the boundary value problem in a domain with a single finite cavity G. The elastic material is characterized by the Lamé constants μ and λ. On ∂G we impose free-traction boundary conditions, and at infinity the uniform shear stress field is specified. The displacement field $\mathbf{u}$ satisfies the following boundary value problem:

$$\nabla\cdot\sigma = 0, \quad \sigma = \mathscr{C} : \varepsilon, \quad \varepsilon = \tfrac{1}{2}(\nabla\mathbf{u} + \nabla\mathbf{u}^T), \quad \mathbf{x}\in\mathscr{B}_\rho\backslash G,$$

$$\sigma^{(n)}(\mathbf{u};\mathbf{x}) = 0, \quad \mathbf{x}\in\partial G,$$

$$\sigma^{(n)}(\mathbf{u};\mathbf{x}) = \sigma^\infty_{ij} n_j, \quad \mathbf{x}\in\partial\mathscr{B}_\rho, \tag{2.1}$$

where σ is the stress tensor, ε is the strain tensor, $\mathscr{C} = \{\mathscr{C}_{ijkl}\}$ is the fourth order tensor of elastic constants, (:) denotes contraction by two indices, $\mathscr{B}_\rho = \{(x,y) : x^2+y^2 < \rho^2\}$ and ρ is sufficiently large, n_j are components of the unit outward normal.

For an isotropic material which we consider here, the above system is reduced to the Lamé equations:

$$\mathscr{L}(\mathbf{u};\mathbf{x}) := \mu\Delta\mathbf{u} + (\lambda+\mu)\nabla\nabla\cdot\mathbf{u} = 0, \quad \mathbf{x}\in\mathscr{B}_\rho\backslash G,$$

$$\sigma^{(n)}(\mathbf{u};\mathbf{x}) = 0, \quad \mathbf{x}\in\partial G,$$

$$\sigma^{(n)}(\mathbf{u};\mathbf{x}) = \sigma^\infty_{ij} n_j, \quad \mathbf{x}\in\partial\mathscr{B}_\rho. \tag{2.2}$$

Following variational technique (see Sokolowski and Zolesio, 1992), we define the energy space $W(\mathscr{B}_\rho)$ for the boundary value problem (2.2) and introduce the norm:

$$\|\mathbf{u}\|^2_W = \frac{1}{2}\int_{\partial\mathscr{B}_\rho} \sigma^\infty_{ij} n_j u_i \,\mathrm{d}s. \tag{2.3}$$

The elastic energy of the region which is bounded by $\partial\mathscr{B}_\rho$ can be evaluated as

$$\mathscr{E}(\mathbf{u};\mathscr{B}_\rho\backslash G) = -\|\mathbf{u}\|^2_W. \tag{2.4}$$

We remark that it can be represented as a difference between the potential energy and the work of external forces.

The solution of the boundary value problem (2.2) minimizes the energy (2.4):

$$\mathscr{E}(\mathbf{u};\mathscr{B}_\rho\backslash G) = \min_{\mathbf{U}} \mathscr{E}(\mathbf{U};\mathscr{B}_\rho\backslash G). \tag{2.5}$$

We define the increment of energy as a difference between two functionals associated with full energy in the homogeneous disk $\mathscr{B}_\rho = \{\mathbf{x} : \|\mathbf{x}\| < \rho\}$ and in the disk $\mathscr{B}_\rho$ weakened by the cavity G:

$$\delta W_{G;\sigma^\infty_{ij}} = \lim_{\rho\to\infty}\{\mathscr{E}(\mathbf{u};\mathscr{B}_r\backslash G) - \mathscr{E}(\mathbf{u}^\infty;\mathscr{B}_r)\}$$

$$= \lim_{\rho\to\infty}\left(-\frac{1}{2}\int_{\mathscr{B}_\rho\backslash G}\sigma_{ij}\varepsilon_{ij}\,\mathrm{d}x + \frac{1}{2}\int_{\mathscr{B}_\rho}\sigma^\infty_{ij}\varepsilon^\infty_{ij}\,\mathrm{d}x\right),$$

$$\mathscr{B}_\rho = \{\mathbf{x} : \|\mathbf{x}\| < \rho\}. \tag{2.6}$$

Here σ^∞_{ij}, ε^∞_{ij} are components of the stress and the strain tensors in the homogeneous disk, and σ_{ij}, ε_{ij} are the stress and strain in the disk $\mathscr{B}_\rho$ with the cavity G.†

2.2. *Optimization problem*

The main objective is to find the shape of the cavity which provides the minimal absolute value of the energy increment. Note that the energy increment is negative for the disk with a cavity. The constraints of the fixed area and boundness of the domain are imposed.

† Note that the boundary value problem is solved in the bounded domain $\mathscr{B}_\rho\backslash G$.

We formulate the optimization problem in the following form: find a bounded domain G^* of a fixed area such that

$$\delta W_{G^*,\sigma_{ij}^\infty} = \max_G \delta W = \max_G \lim_{\rho\to\infty} \left\{ \min_{\mathbf{U}} \mathscr{E}(\sigma_{ij}^\infty ; \mathscr{B}_\rho \backslash G) - \min_{\mathbf{U}} \mathscr{E}(\sigma_{ij}^\infty ; \mathscr{B}_\rho) \right\}, \tag{2.7}$$

where the maximum is taken over all simply connected bounded domains of a given area. Let us now discuss the set of admissible minimizers. An infinite plane with an arbitrary single cavity can be mapped to the exterior of the unit disc by the conformal mapping represented in the form

$$\omega(\xi) = R\left[\frac{1}{\xi} + \sum_{n=1}^{\infty} c_n \xi^n\right], \tag{2.8}$$

where R and c_n are constant coefficients.

The constraint of the fixed area can be written via the conformal mapping coefficients:

$$S(G) = \pi R^2 \left(1 - \sum_{n=1}^{\infty} n|c_n|^2\right) = \text{const.} \tag{2.9}$$

We determine the set of admissible cavities by their coefficients R and c_n of conformal mapping to the unit disc. The optimization problem becomes:

> *Find the set of coefficients* R *and* c_n [*see* (2.8)] *restricted by* (2.9) *that lead to a cavity which minimizes* (2.7).

This formulation corresponds to our goal to find an optimal single-connected cavity, rather than an array of smaller cavities of the same area.

2.3. *Representation of the energy increment*

It is convenient to present the energy increment via "polarization" tensor (see Zorin *et al.*, 1988; Babich *et al.*, 1989) for precise proof of this representation):

$$\delta W = \boldsymbol{\varepsilon} : \mathscr{P} : \boldsymbol{\varepsilon}. \tag{2.10}$$

where $\mathscr{P}_{ijkl}$, $i, j, k, l = 1, 2$ is the 4-th order "polarization" tensor (also see Pólya and Szegö, 1951; Walpole, 1966). It has the same symmetry properties as the Hooke's tensor $\mathscr{C}_{ijkl}$. Namely,

$$\mathscr{P}_{ijkl} = \mathscr{P}_{jikl} = \mathscr{P}_{ijlk} = \mathscr{P}_{klij},$$

and the number of independent elements is six for 2-D geometry. The "polarization" tensor characterizes the remote displacement field associated with the presence of cavity G. If we can specify the constant-strain fields corresponding to the following displacements $\mathbf{V}^{(1)} = (x_1, 0)$, $\mathbf{V}^{(2)} = (0, x_2)$, $\mathbf{V}^{(3)} = 2^{-1/2}(x_2, x_1)$ (biaxial tensile and shear loading at infinity) then the displacement fields in the region $\mathbb{R}^2 \backslash G$ admit the following representation

$$\mathbf{U}^{(i)} = \mathbf{V}^{(i)} + \mathbf{W}^{(i)},$$

and at infinity the "polarization" fields admit the following asymptotic expansions:†

† Repeated indices are regarded to be the indices of summation.

$$\mathbf{W}^{(1)} = \begin{pmatrix} \mathscr{P}_{11nm} T_{n1,m} \\ \mathscr{P}_{11nm} T_{n2,m} \end{pmatrix} + O(|x|^{-2}),$$

$$\mathbf{W}^{(2)} = \begin{pmatrix} \mathscr{P}_{22nm} T_{n1,m} \\ \mathscr{P}_{22nm} T_{n2,m} \end{pmatrix} + O(|x|^{-2}),$$

$$\mathbf{W}^{(3)} = \sqrt{2} \begin{pmatrix} \mathscr{P}_{12nm} T_{n1,m} \\ \mathscr{P}_{12nm} T_{n2,m} \end{pmatrix} + O(|x|^{-2}),$$

where $\mathbf{T}(\mathbf{x})$ is Somigliana tensor, and $T_{IJ,1}$ and $T_{IJ,2}$ denote the derivatives of the component IJ with respect to x_1 or x_2, respectively.

$$\mathbf{T}(\mathbf{x}) = q \begin{bmatrix} -\kappa \ln(x_1^2 + x_2^2) + \dfrac{2x_1^2}{x_1^2 + x_2^2} & \dfrac{2x_1 x_2}{x_1^2 + x_2^2} \\ \dfrac{2x_1 x_2}{x_1^2 + x_2^2} & -\kappa \ln(x_1^2 + x_2^2) + \dfrac{2x_2^2}{x_1^2 + x_2^2} \end{bmatrix}, \quad q = \frac{\lambda + \mu}{8\pi\mu(\lambda + 2\mu)}.$$

The Pólya–Szegö tensor $\|\mathscr{P}\|_{i,j,k,l=1}^2$ (Zorin *et al.*, 1988) characterizes the morphology of the cavity and elastic constants of the material. The tensor $\mathscr{P}$ depends on coefficients R, c_n and elastic constants μ, λ only:

$$\mathscr{P} = \mathscr{P}(R, c_n, \mu, \lambda). \tag{2.11}$$

To obtain explicit approximate formulae for the tensor $\mathscr{P}$ we consider truncation of the expansion (2.8), and keep the first N terms of the series. It allows one to reduce the problem to the solution of the system of N linear algebraic equations.

For example, when $N = 3$ we obtain:†

$$\mathscr{P}_{1111} = -\Omega + \frac{\Sigma}{\kappa - 1} - \frac{\Xi}{(\kappa - 1)^2}, \quad \mathscr{P}_{1122} = \Omega - \frac{\Xi}{(\kappa - 1)^2}, \quad \mathscr{P}_{1212} = \Upsilon,$$

$$\mathscr{P}_{2222} = -\Omega - \frac{\Sigma}{\kappa - 1} - \frac{\Xi}{(\kappa - 1)^2}, \quad \mathscr{P}_{1112} = -\Theta + \frac{\Lambda}{\kappa - 1}, \quad \mathscr{P}_{2212} = \Theta + \frac{\Lambda}{\kappa - 1},$$

where

$$\Omega = \frac{\mathrm{Re}(c_3) + 1}{1 - |c_3|^2}, \quad \Sigma = 4\left[\frac{\mathrm{Re}(c_1)}{1 - |c_3|^2} + \frac{\mathrm{Re}(c_3 \bar{c}_1)}{1 - |c_3|^2}\right],$$

$$\Xi = 2 + 4|c_2|^2 + 6|c_3|^2 + 2|c_1|^2 \frac{1 + |c_3|^2}{1 - |c_3|^2} + \frac{4\,\mathrm{Re}(c_1^2 \bar{c}_3)}{1 - |c_3|^2},$$

$$\Theta = \frac{\mathrm{Im}(c_3)}{1 - |c_3|^2}, \quad \Lambda = 2\left[\frac{\mathrm{Im}(c_1)}{1 - |c_3|^2} + \frac{\mathrm{Im}(c_3 \bar{c}_1)}{1 - |c_3|^2}\right],$$

$$\Upsilon = \frac{\mathrm{Re}(c_3) - 1}{1 - |c_3|^2}.$$

Thus, the mathematical formulation of the optimal problem reduces to the maximization problem for the function of N variables:

† Formulae for arbitrary N were published in Movchan and Serkov (1997).

$$\max_{\substack{c_n, n=1..N \\ \text{area}(G) \text{ is fixed}}} (\boldsymbol{\varepsilon} : \mathscr{P} : \boldsymbol{\varepsilon}). \tag{2.12}$$

2.4. *Necessary conditions of optimality*

The stationarity conditions for the optimal boundary ∂G can be derived using the classical variational scheme (see Courant and Hilbert, 1962). This condition states that the energy density must be constant along the boundary ∂G. For the case of a cavity with zero tractions specified on the boundary, the theorem implies that the only non-zero component of stress $\sigma_{tt} = \boldsymbol{\sigma} : \mathbf{t} \otimes \mathbf{t}$ must be of a constant absolute value on the cavity contour, where $\mathbf{t}$ denotes the unit tangent to the contour.

$$|\sigma_{tt}| = c = \text{const} \quad \text{on an optimal boundary.} \tag{2.13}$$

Applying this condition to our formulation, where a pure shear is prescribed at infinity, we observe that it is impossible to satisfy (2.13), assuming $\sigma_{tt} = \text{const}$.

To resolve this contradiction we have to assume that σ_{tt} is piece-wise constant, taking values c and $-c$. The points of discontinuity of σ_{tt} must correspond to irregularities on the boundary.† Finally, we conclude that an optimal cavity is necessarily bounded by a non-smooth curve.

This observation has been made in the paper by Cherkaev and Vigdergauz (1986), where an optimal shape that has been found numerically looks like a rectangle. In Section 6 below we will compute the angle at the corners using asymptotic analysis.

2.5. *Related optimal composites*

One possible approach to the calculation of the optimal energy of the body with cavities is the following. Consider a periodic structure with cavities, which is characterized by the volume fraction c and by the shape of cavities. The effective compliance tensor $S^*(c)$ of such a structure can be evaluated and we can bound the effective shear and bulk moduli independently of the cavities shape. The bounds (introduced in the papers by Gibiansky and Cherkaev, 1984; Milton, 1990) are proved to be exact, and they correspond to the mentioned "second rank matrix laminates". Suppose that the optimal composite with a small volume fraction $c \ll 1$ of cavities occupies the volume A and has a uniform average stress field σ due to an external loading. The total volume of the cavities is equal to $C = cA$. The energy change associated with the cavity can be computed as

$$\delta W = \left(\sigma : \frac{\hat{c}}{\partial c} S^*(c) \Big|_{c=0} : \sigma \right) cA. \tag{2.14}$$

Using the explicit formula for the energy of the optimal composite derived by Gibiansky and Cherkaev (1984) we can compute the increment:

$$\delta W = \begin{cases} \Upsilon c(\sigma_1 + \sigma_2)^2, & \sigma_1 \sigma_2 \geqslant 0, \\ \Upsilon c(\sigma_1 - \sigma_2)^2, & \sigma_1 \sigma_2 \leqslant 0, \end{cases} \tag{2.15}$$

where $\Upsilon = -(2\mu + \lambda)/(4\mu(\lambda + \mu))$, λ and μ are the Lamé elastic moduli, and σ_1, σ_2 are principal stresses.

It should be emphasized that this approach does not pose any restrictions to the connectness of the cavities, and it turns out that the optimal bounds are achieved on the second rank laminates. Therefore, we could expect that the cost of the optimal problem will be greater when an additional restriction, single-connectness of cavities is imposed.

† Smooth boundary components correspond to a continuous behaviour of σ_{tt}.

3. MINIMIZATION TECHNIQUE

This optimization problem can be reduced to minimization of a function of several variables. The unknown variables are the coefficients of the conformal mapping subject to the restriction $|c_n| < 1/\sqrt{n}$ according to (2.9).

Our purpose is to find the set of conformal mapping coefficients $\{c_n\}$ minimizing the absolute value of the energy increment (2.10). In other words our problem reduces to multi-dimensional minimization of a function f of $2N$ variables (the conformal mapping coefficients are complex).

To do this we use the downhill simplex method [see Numerical Recipes in FORTRAN (1992) and Appendix for more details].

Our calculation confirms that the optimal construction for uniform loading ($\sigma_{11} = \sigma_{22}$) is a circular cavity and the optimal construction for uniaxial loading is a crack oriented along the loading line. For the case of composition of two uniaxial loadings of the same sign, the optimal shape will be an ellipse oriented along the direction corresponding to the maximal principal stress and having the following parameters (Vigdergauz, 1988):

$$\omega(\xi) = R\left[\xi + \frac{(a-b)}{(a+b\xi)}\right], \quad \frac{a}{b} = \frac{\sigma_{11}}{\sigma_{22}}, \tag{3.16}$$

where a and b are semi-axes of the ellipse, and σ_{11}, σ_{22} are principal stresses of the same sign.

The energy increment associated with the optimal elliptical cavity of the unit area can be estimated as (Gibiansky and Cherkaev, 1984)

$$\delta W^{\text{opt}} = -\frac{\lambda+2\mu}{4\mu(\lambda+\mu)}(\sigma_1+\sigma_2)^2. \tag{3.17}$$

The properties of the optimal field for ($\sigma_1\sigma_2 \geqslant 0$) reduce to the constant dilatation (or constant first invariant of the stress tensor) in the exterior domain and the constant tangential stress on the cavity boundary. In the next section we describe our results for the remaining case when $\sigma_1\sigma_2 < 0$.

4. THE MAIN RESULT: THE OPTIMAL SHAPE OF THE CAVITY

In this section we use the complex variable technique to compute the shape of the optimal cavity that gives minimum for the absolute value of the energy increment in the state of shear loading applied at infinity.

First, we apply the minimization procedure referred to Section 3 and present numerical values of the coefficients of the conformal mapping function. Then we use this mapping function and solve the direct elasticity problem for an optimal domain. Finally, the analysis of the inverse problem is presented: we seek the shape of the cavity that provides piecewise constant σ_{tt} on the cavity contour and show the agreement with the results of the optimization procedure of Section 3.

4.1. *Optimization of the shape by the direct method*

Now consider the cavity under the shear loading. The optimal bound for the energy increment is well known (see, for example, Gibiansky and Cherkaev, 1984). It corresponds to the multiply connected laminated composites:

$$\delta W^{\text{opt}} = -\frac{\lambda+2\mu}{4\mu(\lambda+\mu)}[(\sigma_{11}-\sigma_{22})^2+4\sigma_{12}^2]. \tag{4.1}$$

For example, we obtain that the absolute value of the energy increment for a circular cavity is two times greater than the optimal one (4.1). Our aim is to find the geometry of the

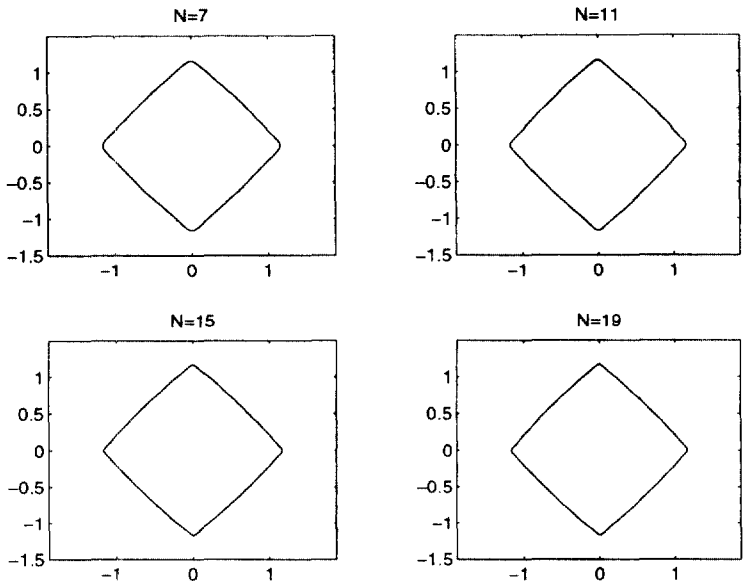

Fig. 1. The shape of the optimal domain.

region, which is specified by a smaller energy change than the circular cavity and which is the best among simply-connected domains.

Using the exact representation for the energy increment (2.10), (2.11) and the formulae below (2.11), together with the minimization procedure, we find in the case of $N = 3$

$$\omega(\xi) = R\left(\frac{1}{\xi} + \frac{\sqrt{2}-1}{3}\xi^3\right). \tag{4.2}$$

Here the constant R is chosen in such a way that the cavity has a unit area.

Increasing the number of terms in (2.8) and taking into account 7, 11, 15 and 19 terms correspondingly, we calculate that non-zero conformal mapping coefficients c_n for the optimal domain (see Fig. 1) have the following approximate values:

The energy increment for such a domain can be specified as

$$\Delta\mathscr{E} = -\mathscr{K}\frac{\sigma_{12}^2(\lambda+2\mu)}{2\mu(\lambda+\mu)}, \tag{4.3}$$

where the coefficient $\mathscr{K}$ is given in Table 2 as a function of the number N of conformal mapping coefficients.

For a circular cavity under pure shear the coefficient $\mathscr{K}$ in formula (4.3) is equal to four, while the absolute minimum value is two, as evidenced by (4.1).

Table 1. Coefficients of the conformal mapping obtained by the optimization procedure

Coefficients	$N = 19$	$N = 15$	$N = 11$	$N = 7$	$N = 3$
c_3	0.14445	0.14420	0.14372	0.14251	0.13814
c_7	0.01699	0.01683	0.01652	0.01575	
c_{11}	0.00552	0.00539	0.00513		
c_{15}	0.00250	0.00239			
c_{19}	0.00133				

Table 2. The dependence of $\mathscr{K}$ on the number of coefficients in the conformal mapping series

The number of coefficients N	Coefficient $\mathscr{K}$
3	3.72792
7	3.71725
11	3.71532
15	3.71473
19	3.71449

We can see (Fig. 1) that by increasing the number of coefficients the optimal domain approaches what looks like a square.

Note that an interesting case arises for non-pure shear. We find that the optimal cavity is close to a rectangular one with the sides ratio given in Fig. 2. The ratio of the energy increment and the optimal energy (4.1) is presented in Fig. 3. We see that simply connected inclusions (holes) stop being optimal when $\sigma_1\sigma_2 < 0$.

4.2. *Properties of the optimal hole*

In this section we use Kolosov–Muskhelishvili potentials ϕ and ψ to represent elastic fields in the exterior of the hole (Muskhelishvili, 1953). The displacement vector $[u_1, u_2]$ is given by

$$u_1 + iu_2 = \left(\frac{1}{k} + \frac{1}{2\mu}\right)\varphi(z) - \frac{1}{2\mu}(\bar{\psi}(z) + z\bar{\Phi}(z)), \quad k = \lambda + \mu, \tag{4.4}$$

where $\Phi = \varphi'$. The associated stress $\boldsymbol{\sigma} = \mathscr{C}:\varepsilon$ is given by

$$\begin{aligned} \sigma_{11} + \sigma_{22} &= 4\,\mathrm{Re}\,\Phi(z), \\ \sigma_{22} - \sigma_{11} + 2i\sigma_{12} &= 2(\bar{z}\Phi'(z) + \Psi(z)), \end{aligned} \tag{4.5}$$

where $\Psi = \psi'$.

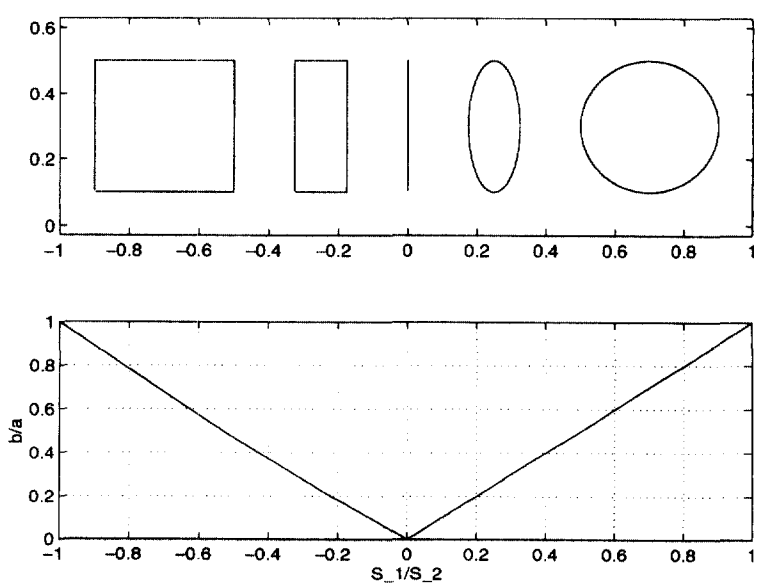

Fig. 2. Geometry of the optimal cavity as the function of applied stresses.

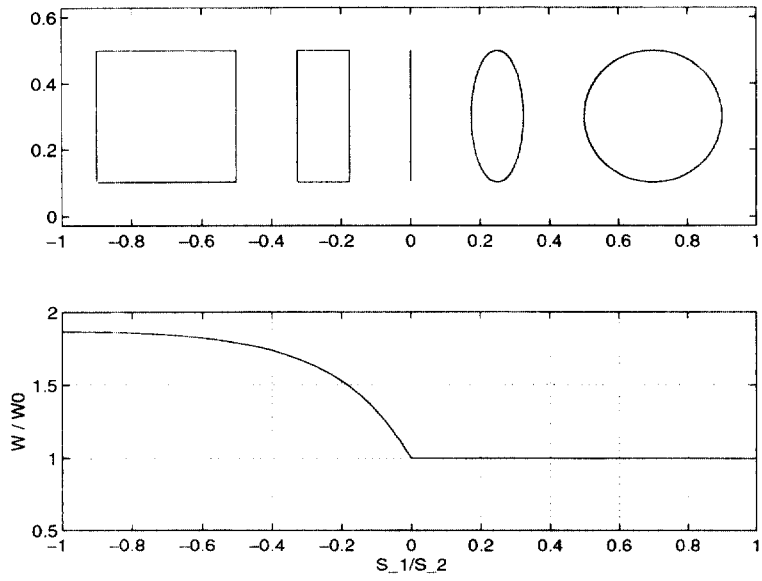

Fig. 3. The normalized energy change versus applied stress.

For the conformal image of the unit disk under the mapping $\omega(\xi)$ given by (2.8) with coefficients from Table 1 the representation for complex potentials can be obtained from the analysis of the Kolosov–Muskhelishvili integral equation:

$$\frac{1}{2\pi i}\oint_{\gamma}\frac{\varphi(\sigma)}{\sigma-\xi}\,d\sigma+\frac{1}{2\pi i}\oint_{\gamma}\frac{\omega(\sigma)\overline{\varphi'(\sigma)}}{\overline{\omega(\xi)}(\sigma-\xi)}\,d\sigma-i\sigma_{12}R\xi=0, \tag{4.6}$$

where γ is the unit circle. Omitting technical calculations we write the series representation for the complex potential $\varphi(\xi)$

$$\varphi(\xi)=\sum_{m=1}^{N}\beta_m\xi^m, \quad |\xi|\leqslant 1, \tag{4.7}$$

where the coefficients β_m solve the linear system:

$$\beta_m-\sum_{n=1}^{N-m-1}\rho_{N-m-n-1}n\bar{\beta}_n-i\sigma'_{12}R\delta_{m1}=0, \quad m=\overline{1,N},$$

where

$$\rho_k=\frac{1}{k!}\frac{d^k}{d\xi^k}\left[\frac{\xi^{N+1}+\Sigma_{n=1}^{N}c_n\xi^{N-n}}{1-\Sigma_{n=1}^{N}n\bar{c}_n\xi^{n+1}}\right]\Bigg|_{\xi=0}.$$

Note, that in our particular case the symmetry conditions yield that all non-zero conformal mapping coefficients have indices $4n-1$, $n=1,2,3,\ldots$ They correspond to non-zero coefficients β_{4n+1}, $n=1,2,3,\ldots$, and all remaining coefficients vanish.

The complex potential $\psi(\xi)$ admits the representation:

$$\psi(\xi)=i\sigma'_{12}R\frac{1}{\xi}-\frac{\omega(1/\xi)\varphi'(\xi)}{\omega'(\xi)}-\sum_{m=0}^{N}\sum_{n=1}^{N-m-1}\bar{\rho}_{N-m-n-1}n\beta_n\frac{1}{\xi^m}. \tag{4.8}$$

Note that the complex potential $\psi(\xi)$ has only a simple pole at the origin [look at the first

term in representation (4.8)]. At the same time the third term in (4.8) compensates the singular part from the second term, resulting in ψ having the pole of order one only.

For example, for $N = 3$ we obtain

$$\varphi(\xi) = \frac{3}{2+\sqrt{2}} i\sigma_{12}^{\infty} R\xi, \quad |\xi| \leqslant 1;$$

$$\psi(\xi) = iR\sigma_{12}^{\infty}\left(\frac{1}{\xi} + \frac{\xi^3(6-2\sqrt{2})}{(2+\sqrt{2})(\xi^4(1-\sqrt{2})+1)}\right). \tag{4.9}$$

Taking into account the representation for stress components via the complex potentials:

$$\sigma_{11}+\sigma_{22} = 2\left(\frac{\varphi'(\xi)}{\omega'(\xi)} + \overline{\frac{\varphi'(\xi)}{\omega'(\xi)}}\right),$$

$$\sigma_{22}-\sigma_{11}+2i\sigma_{12} = 2\left(\overline{\omega(\xi)}\frac{\varphi''(\xi)\omega'(\xi)-\varphi'(\xi)\omega''(\xi)}{\omega'(\xi)^3} + \frac{\varphi'(\xi)}{\omega'(\xi)}\right), \tag{4.10}$$

we calculate the hydrostatic $\{\sigma_{11}+\sigma_{22}\}$ and deviatoric $\{(\sigma_{22}-\sigma_{11})^2+4\sigma_{12}^2\}$ parts of the stress tensor. In Figs 4–6 the first invariant, the deviatoric part and the energy density are presented for the domain described by (4.2).

Using (4.7) and (4.8) we calculate the tangential stress σ_{tt} on the boundary for a different number of terms in the conformal mapping function (Table 1). The results are presented in Fig. 7 for $N = 7, 11, 15, 19$. It is possible to see that the modulus of the tangential stress is constant along the contour except in the small neighbourhood of corners, where it vanishes, and the diameter of this neighbourhood vanishes as we increase N. This observation confirms that the necessary condition of optimality (2.13) is satisfied for our domain under pure shear.

Now we are going to look at the corners of our optimal hole. The Christoffel–Schwartz integral (Savin, 1961)

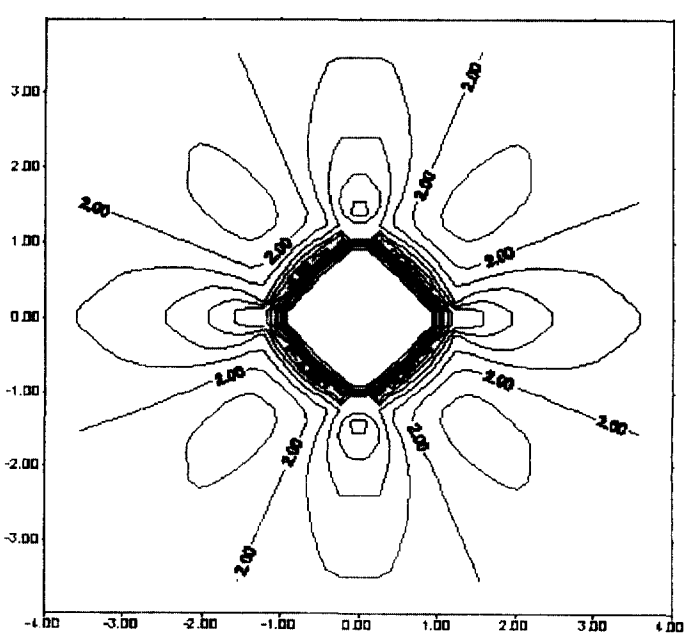

Fig. 4. The distribution of the energy density for the optimal domain.

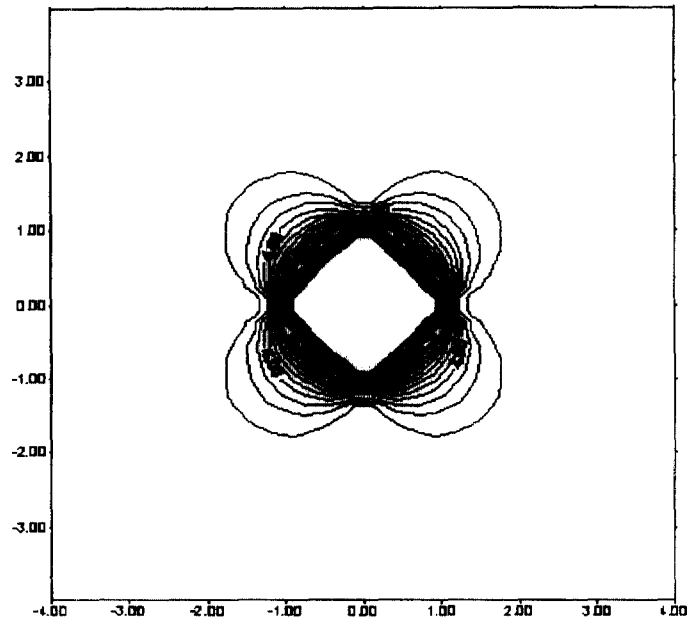

Fig. 5. The distribution of the first invariant of the stress tensor for the optimal domain.

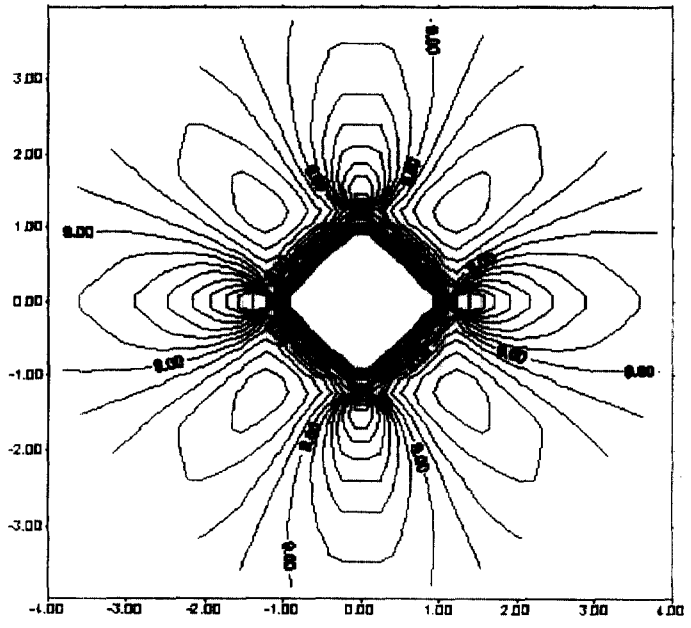

Fig. 6. The distribution of the deviatoric part of the stress tensor for the optimal domain.

$$\omega(\xi) = R\int_1^{\xi} \frac{\sqrt{t^4-1}}{t^2}\,\mathrm{d}t = R\left(\frac{1}{\xi} + \frac{\xi^3}{6} + \frac{\xi^7}{56} + \frac{\xi^{11}}{176} + \frac{\xi^{15}}{384} + \frac{7\xi^{19}}{4864} + \cdots\right)$$

$$= R\left(\frac{1}{\xi} + 0.16667\xi^3 + 0.01786\xi^7 + 0.00568\xi^{11} + 0.00260\xi^{15} + \cdots\right)$$

specifies the mapping of the unit disk to the exterior of a square.

The slightly modified conformal mapping

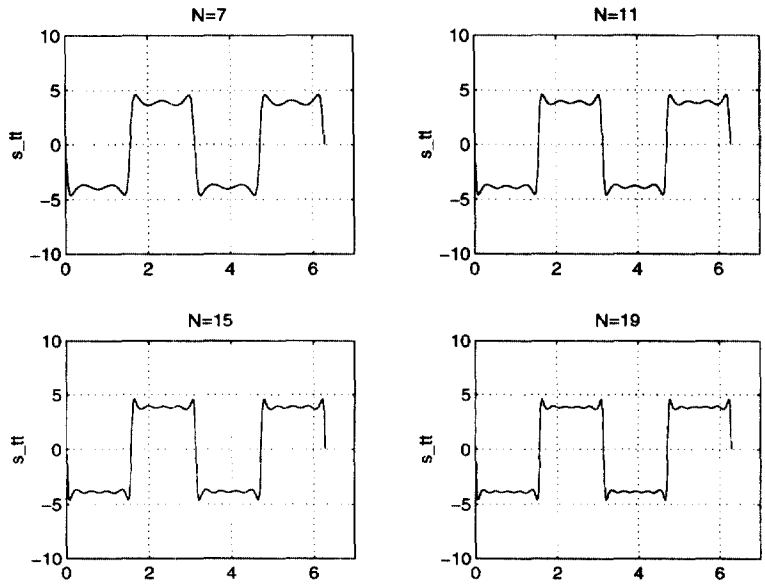

Fig. 7. The tangential stress on the boundary.

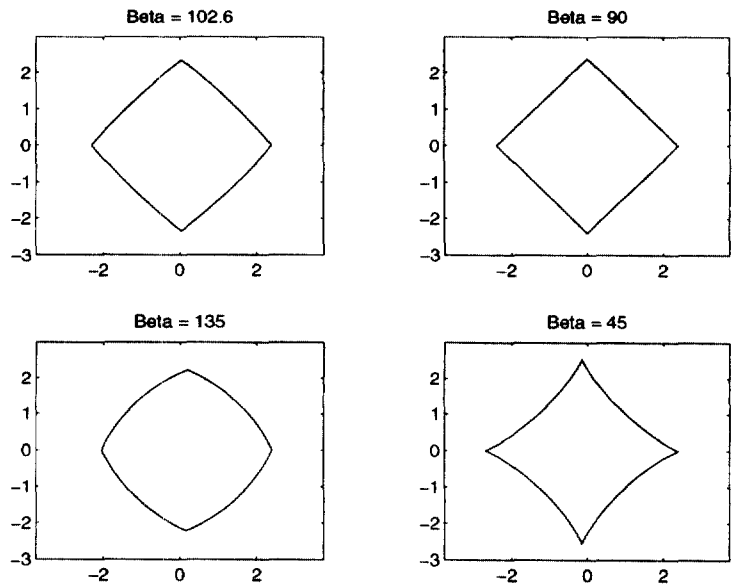

Fig. 8. The regions obtained by the conformal mapping.

$$\omega(\xi) = R\int_1^{\xi} \frac{(t^4-1)^{\alpha}}{t^2}\,\mathrm{d}t, \quad \alpha = 1-\beta\pi^{-1}, \tag{4.11}$$

where β is different from $\pi/2$, corresponds to a transformation of the unit disk to a symmetric domain with the angle β near the corners (see Fig. 8). The opening angle near the vertex of the point $\xi = 1$ can be calculated as

$$\beta = \pi - [arg\,\omega'(\xi)|_{\xi\to 1-0i} - arg\,\omega'(\xi)|_{\xi\to 1+0i}]$$

$$= \pi - \left(\lim_{\xi\to 1-0i}\frac{(t^4-1)^{\alpha}}{t^2} - \lim_{\xi\to 1+0i}\frac{(t^4-1)^{\alpha}}{t^2}\right) = \pi - \left(\frac{3\pi\alpha}{2} - \frac{\pi\alpha}{2}\right).$$

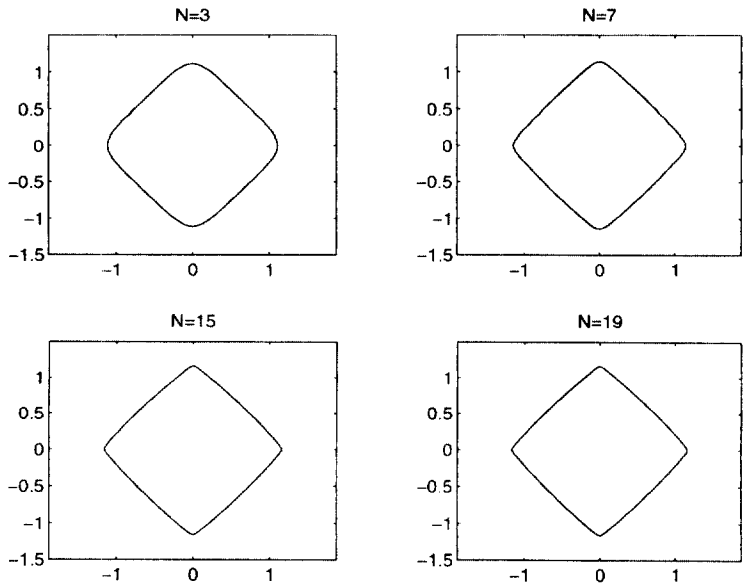

Fig. 9. The shape of domainb with piecewise constant tangential stresses on the boundary.

The remaining three angles (near the points $\xi = i, -1, -i$) have the same values. Changing β we can find the conformal mapping function which will be in good agreement with the results of the optimization procedure. If we choose $\beta_* = 102.6^\circ$ then (4.11) can be rewritten in the form

$$\omega(\xi) = R\left(\frac{1}{\xi} + 0.14343\xi^3 + 0.01751\xi^7 + 0.00585\xi^{11} + 0.00275\xi^{15} + \cdots\right),$$

which agrees with Table 1. It suggests that the quantity β_* is the critical angle in the Carothers problem (Sternberg and Koiter, 1958) (more detailed discussion will be presented in Section 6, where we will show that this is not an accidental agreement).

5. THE SOLUTION OF THE INVERSE PROBLEM

The objective of this section is to solve an inverse problem: to find the shape of the quadrilateral G from the condition $\sigma_{tt} = c$ or $-c$ on the boundary. Here we do not refer to the energy evaluation. However, we demonstrate that the results of two approaches coincide.

We start with the Kolosov–Muskhelishvili representation of the boundary condition

$$\boldsymbol{\sigma}^{(n)}(\mathbf{u}; \mathbf{x}) = 0, \quad \mathbf{x} \in \partial G$$

for complex potentials φ and ψ

$$\varphi(z) + z\overline{\varphi'(z)} + \overline{\psi(z)} = 0, \quad z \in \partial G. \tag{5.1}$$

Under the pure shear loading

$$\varphi(z) \to 0, \quad |z| \to \infty$$
$$\psi(z) \to i\sigma_{12}z, \quad |z| \to \infty.$$

After mapping the exterior of G onto the interior of the unit disk by the conformal mapping $z = \omega(\xi)$ we can rewrite the integral equation (4.6) for the potential φ

$$\varphi(\xi) + \frac{1}{2\pi i}\oint_{\gamma} \frac{\omega(\sigma)\overline{\Phi(\sigma)}}{\sigma - \xi} d\sigma - i\sigma_{12} R\xi = 0, \tag{5.2}$$

where $\Phi(\sigma) = [\varphi'(\sigma)/\omega'(\sigma)]$ and $\omega(\sigma)$ is the conformal mapping function. The boundary of unit disk is denoted by γ.

Now we can apply the condition of the piece wise constant tangential stresses on the boundary. The $1, i, -1, -i$ in the ξ-plane map to the corners of the domain G in z-plane. So conditions (2.13) can be rewritten as

$$\sigma_{tt} = 4 \operatorname{Re} \varphi'(z) = 4 \operatorname{Re} \Phi(\xi) = \pm 4A, \quad z \in \partial G, \tag{5.3}$$

where $c = 4A$ is an unknown constant. The unit circle $|\xi| = 1$ is the image of the boundary, therefore:

$$\operatorname{Re} \Phi(e^{i\alpha}) = \begin{cases} A, & \alpha \in \left(0, \frac{\pi}{2}\right) \cup \left(\pi, \frac{3\pi}{2}\right) \\ -A, & \alpha \in \left(\frac{\pi}{2}, \pi\right) \cup \left(\frac{3\pi}{2}, 2\pi\right) \end{cases}. \tag{5.4}$$

Using the Schwartz formula that recovers the holomorphic function in the unit disk by the values of its real part on the boundary, we obtain

$$\Phi(\xi) = \frac{2}{\pi} Ai \ln \frac{1 - \xi^2}{1 + \xi^2}, \quad |\xi| \leqslant 1. \tag{5.5}$$

Therefore, expression (5.5) is the explicit representation for the complex potential $\Phi(\xi)$ satisfying the condition (2.13).

Take the derivative of (5.2), and use the identity $\overline{\Phi(\sigma)} = 2 \operatorname{Re} \Phi(\sigma) - \Phi(\sigma)$ and the expression for the derivative of the Cauchy integral. The integral equation (5.2) reduces to

$$\Phi(\xi)\omega'(\xi) + \frac{1}{\pi i}\oint_{\gamma} \frac{\omega(\sigma) \operatorname{Re} \Phi(\sigma)}{(\sigma - \xi)^2} d\sigma - \frac{1}{2\pi i}\oint_{\gamma} \frac{\omega(\sigma)\Phi(\sigma)}{(\sigma - \xi)^2} d\sigma = \frac{1}{2} R \operatorname{dev} \boldsymbol{\sigma}^{\infty}, \tag{5.6}$$

where $\operatorname{dev} \boldsymbol{\sigma} = \sigma_{22} - \sigma_{11} + 2i\sigma_{12}$.

Using the expression for the real part of the potential $\Phi(\xi)$ (5.4) and formulae for the derivatives of the Cauchy integral, we can represent the integrals on the left in the following way:

$$\frac{1}{2\pi i}\oint_{\gamma} \frac{\omega(\sigma)\Phi(\sigma)}{(\sigma - \xi)^2} d\sigma = \frac{d}{d\xi} \{\omega(\xi)\Phi(\xi)\}$$

and

Table 3. Coefficients of conformal mapping obtained as the solution of the inverse problem

	$N = 100$	$N = 19$	$N = 15$	$N = 11$	$N = 7$	$N = 3$
c_3	0.14484	0.13940	0.13759	0.13448	0.12825	0.11111
c_7	0.01727	0.01511	0.01437	0.01306	0.01034	
c_{11}	0.00575	0.00435	0.00385	0.00288		
c_{15}	0.00271	0.00164	0.00119			
c_{19}	0.00152	0.00061				

$$\frac{1}{2\pi i}\oint_{\gamma}\frac{\omega(\sigma)\,\mathrm{Re}\,\Phi(\sigma)}{(\sigma-\xi)^2}\,\mathrm{d}\sigma=\frac{A}{2\pi i}\left(\int_1^i\frac{\omega(\sigma)}{(\sigma-\xi)^2}\,\mathrm{d}\sigma-\int_i^{-1}\frac{\omega(\sigma)}{(\sigma-\xi)^2}\,\mathrm{d}\sigma\right.$$

$$\left.+\int_{-1}^{-i}\frac{\omega(\sigma)}{(\sigma-\xi)^2}\,\mathrm{d}\sigma-\int_{-i}^{1}\frac{\omega(\sigma)}{(\sigma-\xi)^2}\,\mathrm{d}\sigma\right)=\frac{4iA\omega(1)}{\pi(\xi^4-1)}$$

$$+\frac{A}{2\pi i}\left(\int_1^i\frac{\omega'(\sigma)}{\sigma-\xi}\,\mathrm{d}\sigma-\int_i^{-1}\frac{\omega'(\sigma)}{\sigma-\xi}\,\mathrm{d}\sigma+\int_{-1}^{-i}\frac{\omega'(\sigma)}{\sigma-\xi}\,\mathrm{d}\sigma-\int_{-i}^{1}\frac{\omega'(\sigma)}{\sigma-\xi}\,\mathrm{d}\sigma\right).$$

After some lengthy but simple calculations using the symmetry

$$\omega(i)=-i\omega(1),\quad \omega(-1)=-\omega(1),\quad \omega(-i)=i\omega(1),$$

and the Cauchy formula for the holomorphic function in the unit disk we obtain the integral equation for the unknown function $\omega(\xi)$:

$$\frac{8i}{\pi(1-\xi^4)}(\xi\omega(\xi)-\omega(1))-2\left(\omega'(\xi)+\frac{R}{\xi^2}\right)+\frac{2}{\pi i}\int_1^i\frac{\omega'(\sigma)}{\sigma-\xi}\,\mathrm{d}\sigma$$

$$+\frac{2}{\pi i}\int_{-1}^{-i}\frac{\omega'(\sigma)}{\sigma-\xi}\,\mathrm{d}\sigma=\frac{1}{2A}R\,\mathrm{dev}\,\boldsymbol{\sigma}^{\infty},\qquad(5.7)$$

where the integrals are taken over the quarter arcs of the unit circle located in the first and third quadrants respectively.

Now we represent the conformal mapping function ω by the Laurent expansion about the origin:

$$\omega(\xi)=R\left(\frac{1}{\xi}+c_3\xi^3+c_7\xi^7+c_{11}\xi^{11}+c_{15}\xi^{15}+\cdots\right).\qquad(5.8)$$

Integrands in (5.7) can be expanded in a series of different powers of ξ: $[\omega'(\sigma)/(\sigma-\xi)]=\Sigma_{n=0}^{\infty}[\omega'(\sigma)/\sigma^{n+1}]\,\xi^n$. The function $\xi\omega(\xi)/(1-\xi^4)$ can be expressed as the Taylor series as well. After integration† of each term of the series separately and collecting the coefficients near the same powers of ξ we obtain the following linear system of equations for coefficients c_{4m-1}, $m=1\ldots N$:

$$\sum_{m=1}^{N}\frac{2(4m-1)}{2(m-n)-1}c_{4m-1}-4\sum_{m=n+1}^{N}c_{4m-1}+\frac{2}{2n+1}=0,\quad n=1\ldots N.\qquad(5.9)$$

In Table 3 we show the values of conformal mapping coefficients c_m for different N and note that those data are consistent with Table 1.

† The path of integration can be split into two parts: along real axis from 1–0 and along imaginary axis from 0 to i for the first integral and from -1–0 plus from 0 to $-i$ for the second integral.

The next section is devoted to investigation of the domain boundary near the corner. We show that the corner angle is equal to the critical Carothers value (see Sternberg and Koiter, 1958; Markenscoff, 1994).

6. THE ASYMPTOTIC EXPANSION OF THE OPTIMAL SOLUTION NEAR THE CORNERS

The results of the previous section lead to sharp corners on the boundary, provided that we keep all the terms of the series expansion of the conformal mapping. Any finite series corresponds to an analytical boundary of the cavity. Thus, we need a different technique to deal with the fields near the assumed corners on the boundary of the optimal cavity and we need to demonstrate that the necessary conditions are satisfied almost everywhere.

Consider the infinite plane with the corner point and the opening angle close to $\pi/2$. Such situations can explain the behaviour of the conformal mapping function $\omega(\xi)$ near the corners. The components of the stress field in polar coordinates associated with the corner point can be represented via Airy stress function $\Phi(r,\theta)$ (Muskhelishvili, 1953):

$$\sigma_{rr}=\frac{1}{r^2}\frac{\partial^2\Phi}{\partial\theta^2}+\frac{1}{r}\frac{\partial\Phi}{\partial r},\quad \sigma_{\theta\theta}=\frac{\partial^2\Phi}{\partial r^2},\quad \sigma_{r\theta}=-\frac{1}{r}\frac{\partial^2\Phi}{\partial r\,\partial\theta}+\frac{1}{r^2}\frac{\partial\Phi}{\partial\theta}. \tag{6.1}$$

The solution of equilibrium equations in the infinite plane with corner point can be characterized by Airy function of the following structure (Williams, 1952):

$$\Phi=r^{\Lambda_i+1}\{b_1\sin(\Lambda_i+1)\theta+b_2\sin(\Lambda_i-1)\theta+b_3\cos(\Lambda_i+1)\theta+b_4\cos(\Lambda_i-1)\theta\}, \tag{6.2}$$

where the eigenvalues Λ_i are uniquely defined by the corner opening and boundary conditions. For the case of homogeneous traction boundary conditions they can be calculated as the roots of the equation

$$\sin 2\alpha\Lambda=\pm\Lambda\sin 2\alpha, \tag{6.3}$$

where $2\pi-2\alpha$ is the corner opening. We are interested in the solutions Λ of (6.3) that lie in $(0,1]$. For the corner openings from the interval $(0,\pi)$ ($\alpha\in(\pi/2,\pi)$) there are at most three solutions $\Lambda_1<\Lambda_2\leqslant\Lambda_3=1$ in interval $(0,1]$. For detailed analysis of the corresponding eigenvalue problem we refer to Karp and Karal (1962).†

The Air function corresponding to the first eigenvalue has the form

$$\Phi^{(1)}\sim r^{\Lambda_1+1}\left\{\cos(\Lambda_1+1)\theta-\frac{\cos(\Lambda_1+1)\alpha}{\cos(\Lambda_1-1)\alpha}\cos(\Lambda_1-1)\theta\right\}$$

and satisfies the free-traction boundary conditions on the edges of the corner ($\theta=\pm\alpha$). The corresponding displacement field in the polar coordinate system can be represented as

$$\mathbf{u}^{(1)}\sim r^{\Lambda_1}\begin{bmatrix}\cos(\Lambda_1+1)\theta+\dfrac{(\kappa-\Lambda_1)\cos(\Lambda_1+1)\alpha}{(\Lambda_1+1)\cos(\Lambda_1-1)\alpha}\cos(\Lambda_1-1)\theta\\ -\sin(\Lambda_1+1)\theta+\dfrac{(\kappa+\Lambda_1)\cos(\Lambda_1+1)\alpha}{(\Lambda_1+1)\cos(\Lambda_1-1)\alpha}\sin(\Lambda_1-1)\theta\end{bmatrix}, \tag{6.4}$$

where

† For example, when $\alpha=(3\pi/4)$ corresponding to opening 90°, there are three real eigenvalues $\Lambda_1=0.54448$, $\Lambda_2=0.90853$ and $\Lambda_3=1$ in the interval $(0,1]$.

$$\kappa = \frac{\lambda + 3\mu}{\lambda + \mu}.$$

These vectors describe the symmetric part of the displacement field. In other words the displacement component u_r is an even function and the displacement component u_θ is an odd function of θ:

$$\Phi^{(2)} \sim r^{\Lambda_2+1}\left\{\sin(\Lambda_2+1)\theta - \frac{\sin(\Lambda_2+1)\alpha}{\sin(\Lambda_2-1)\alpha}\sin(\Lambda_2-1)\theta\right\},$$

and the corresponding displacement field in the polar coordinate system has a form

$$\mathbf{u}^{(2)} \sim r^{\Lambda_2}\begin{bmatrix} \sin(\Lambda_2+1)\theta + \dfrac{(\kappa-\Lambda_2)\sin(\Lambda_2+1)\alpha}{(\Lambda_2+1)\sin(\Lambda_2-1)\alpha}\sin(\Lambda_2-1)\theta \\ \cos(\Lambda_2+1)\theta - \dfrac{(\kappa+\Lambda_2)\sin(\Lambda_2+1)\alpha}{(\Lambda_2+1)\sin(\Lambda_2-1)\alpha}\cos(\Lambda_2-1)\theta \end{bmatrix} \tag{6.5}$$

and represents a skew-symmetric field (u_r is odd and u_θ is even).

Our interest is in the displacement field corresponding to the second eigenvalue Λ_2 (skew-symmetric field). Only this field will occur in the vicinity of the corner under the shear loading at infinity because of the symmetry of our problem. The displacement field (6.5) produces singularity at the vertex of corner and the non-zero radial stress component on the boundary

$$\sigma_{rr} \sim \pm 4\Lambda_2 r^{\Lambda_2-1}\sin(\Lambda_2+1)\alpha. \tag{6.6}$$

Our intention is to find the situation when the singularity vanishes. We note that the third eigenvalue $\Lambda_3 = 1$ produces zero stress field. The free-traction conditions lead to b_1, b_2, b_3, b_4 being equal to zero in (6.2). The displacement field corresponding to this situation is the rigid body rotation field:

$$\mathbf{u}^{(3)} \sim \begin{pmatrix} 0 \\ r \end{pmatrix}. \tag{6.7}$$

It is similar to the situation which occurs in the problem of the optimal cavity. There is no singularity in the vertex of the corner from inside. From outside, if we apply the external stress field (shear loading) that does not vanish at infinity

$$\boldsymbol{\sigma} = \begin{pmatrix} 0 & \sigma_{12} \\ \sigma_{12} & 0 \end{pmatrix},$$

then the radial stress component on the boundary can be found as

$$\sigma_{rr} = \pm\sigma_{12}\sin 2\alpha. \tag{6.8}$$

It characterizes the piecewise constant function and agrees with the optimality criterion formulated in the previous sections. Matching (6.6) and (6.8), we see that we need $\Lambda_2 = 1$. In this case the singularity in (6.6) disappears. Observe that by decreasing the angle α from 0.75π (corner opening 90°) to $\alpha^* = 0.715\pi$ (corner opening 102.6°), we obtain that the second eigenvalue indeed approaches one (see Karp and Karal, 1962). The precise value of this angle can be found as the solution of the following transcendental equation:

$$\tan 2\alpha^* = 2\alpha^*. \tag{6.9}$$

For $\alpha \leqslant \alpha^*$ and a skew-symmetric loading there is no singularity near the vertex of the corner, the singularity in radial stress component in (6.6) vanishes. For a skew-symmetric loading the opening $2(\pi - \alpha^*) = 102.6^\circ$ is the critical one (Sternberg and Koiter, 1958).

Thus, we have shown that the singularity in stress is absent near the optimal cavity contour for the present case of external shear loading.

Acknowledgements—The authors would like to thank Prof. G. W. Milton for valuable discussions. A.V.C. gratefully acknowledges the support from the National Science Foundation through the grant DMS-9625129. S.K.S. acknowledges the financial support of Bath University. Both A.B.M. and S.K.S. are grateful to the University of Utah for financial support and provision of computer facilities. Finally, our thanks are due to Prof. S. B. Vigdergauz for reading the manuscript and useful comments.

REFERENCES

Avellaneda, M., Cherkaev, A. V., Gibiansky, L. V., Milton, G. W. and Rudelson, M. (1996) A complete characterization of the possible bulk and shear moduli of planar polycrystals. *Journal of the Mechanics and Physics of Solids* **44**(7), 1179–1218.

Babich, V. M., Zorin, I. S., Ivanov, M. I., Movchan, A. B. and Nazarov, S. A. (1989) Integral characteristics in problems of elasticity (in Russian). Steklov Mathematical Institute (LOMI), preprint P-6-89. Leningrad.

Bendsoe, M. P. (1995) Optimization of structural topology, shape, and material. Springer, Berlin, New York.

Carothers, S. D. (1912) Plane strain in a wedge. *Proceedings of the Royal Society, Edinburgh* **23**, 292.

Chenais, D. (1975) On the existence of a solution in a domain identification problem. *Journal of Mathematical Analysis and Applications* **52**, 189–219.

Cherepanov, G. P. (1974) Inverse problems of the plane theory of elasticity. *Applied Mathematics and Mechanics (PMM)* **38**(6), 915–930.

Cherkaev, A. V. and Vigdergauz, S. B. (1986) A hole in a plate, optimal for its biaxial extension–compression. *Applied Mathematics and Mechanics (PMM)* **50**(3), 401–404.

Courant, R. and Hilbert, D. (1962) *Methods of Mathematical Physics*. Interscience Publishers, NY.

Gibiansky, L. V. and Cherkaev, A. V. (1984) Design of composite plates of extremal rigidity. In: *Topics in the Mathematical Modelling of Composite Materials*, ed. A. Cherkaev and R. Kohn. Birhausen, NY.

Gibiansky, L. V. and Cherkaev, A. V. (1993) Microstructures of composites of extremal rigidity and exact estimates of provided energy density. In: *Topics in the Mathematical Modelling of Composite Materials*, ed. A Cherkaev and R. Kohn. Birkhausen, NY, 1997.

Grabovsky, Y. and Kohn, R. V. (1995) Microstructures minimising the energy of a two phase elastic composite in two space dimensions. II: The Vigdergauz microstructure. *Journal of Mechanics and Physics of Solids* **43**(6), 949–972.

Haug, E. J., Choi, K. K. and Komkov, V. (1986) Design sensitivity analysis of structural system. In *Mathematics in Science and Engineering*, Vol. 177. Academic Press, Inc.

Karp, S. N. and Karal, F. C. (1962) The elastic-field behaviour in the neighbourhood of a crack of arbitrary angle. *Communications on Pure and Applied Mathematics* **15**, 413–421.

Kohn, R. V. and Strang, G. (1986) Optimal design and relaxation of variational problems. *Comm. Pure Appl. Math.* **39**, 113–137, 139–182, 353–377.

Markenscoff, X. (1994) Some remarks on the wedge paradox and Saint-Venant's principle. *Journal of Applied Mechanics* **61**, 519–523.

Milton, G. W. (1986) Modelling the properties of composites by laminates. In *Homogenization and Effective Moduli of Materials and Media*, ed. J. L. Ericksen, D. Kinderlehrer, R. Kohn and J.-L. Lions. Springer-Verlag, New York, 150–174.

Milton, G. W. (1990) On characterizing the set of possible effective tensors of composites: The variational method and the translation method. *Communications on Pure and Applied Mathematics* **43**, 63–125.

Movchan, A. B. (1992) Integral characteristics of elastic inclusions and cavities in the two-dimensional theory of elasticity. *European Journal of Applied Mathematics* **3**, 21–30.

Movchan, A. B. and Movchan, N. V. (1995) *Mathematical Modelling of Solids with Nonregular Boundaries*. CRC Press.

Movchan, A. B. and Serkov, S. K. (1991) Elastic polarisation matrices for polygonal domains. *Mechanics of Solids* (English translation of *Izv. AN SSSR. Mekhanika Tverdogo Tela*) **26**(3), 63–68.

Movchan, A. M. and Serkov, S. K. (1997) The Pólya–Szegö matrices in asymptotic models of dilute composites. *European Journal of Applied Mathematics*, **8**, 595–621.

Muskhelishvili, N. I. (1953) *Some Basic Problems of the Mathematical Theory of Elasticity*. Noordhoff, Groningen.

Numerical Recipes in FORTRAN (1992) *The Art of Scientific Computing*, 2nd edn. Cambridge University Press.

Olhoff, N. and Rozvany, G. I. N. (ed). (1995) *First World Congress of Structural and Multidisciplinary Optimization*. Pergamon.

Pironneau, O. (1984) *Optimal Shape Design for Elliptic Systems*. Springer-Verlag.

Prager, W. (1968) Optimality criteria in structural design. *Proceedings of the National Academy of Natural Science, U.S.A.* **61**(3), 794–796.

Pólya, G. and Szegö, G. (1951) *Isoperimetric Inequalities in Mathematical Physics*. Princeton University Press.

Rozvany, G. I. N., Bendsoe, M. P. and Kirsch, U. (1994) Layout optimization of structures. *Appl. Mech. Rev.* **48**(2), 41–119; Addendum: *Appl. Mech. Rev.* **49**(1), 54.

Savin, G. N. (1961) *Stress Concentration Around Holes*. Pergamon Press, New York.

Schnack, E. and Spörl, U. (1986) A mechanical dynamic programming algorithm for structure optimization. *International Journal for Numerical Methods in Engineering* **23**(11), 1985–2004.
Sokolowski, J. and Zolesio, J.-P. (1992) Introduction to shape optimization. *Shape Sensitivity Analysis*. Springer-Verlag.
Sternberg, E. and Koiter, W. T. (1958) The wedge under a concentrated couple: a paradox in the two-dimensional theory of elasticity. *Journal of Applied Mechanics*, pp. 575–581.
Taylor, G. I. (1928) The energy of a body moving in an infinite fluid, with an application to airships. *Proceedings of the Royal Society of London, A* **120,** 13–21.
Vigdergauz, S. B. (1976) Integral equation of the inverse problem of the plane theory of elasticity. *Applied Mathematics and Mechanics (PMM)* **40**(3), 518–521.
Vigdergauz, S. B. (1988) Stressed state of an elastic plane with constant-stress holes. *Mechanics of Solids* (English translation of *Izv. AN SSSR. Mekhanika Tverdogo Tela*) **23**(3), 96–99.
Vigdergauz, S. B. (1989) Piecewise-homogeneous plates of extremal stiffness, *Applied Mathematics and Mechanics (PMM)* **53**(1), 76–80.
Vigdergauz, S. (1994) Two-dimensional grained composites of extreme rigidity, *Journal of Applied Mechanics* **61**(6), 390–394.
Walpole, L. J. (1966) On bounds for the overall elastic moduli of inhomogeneous systems—I. *Journal Mechanics and Physics of Solids* **14,** 151–162.
Williams, M. L. (1952) Stress singularities resulting from various boundary condition in angular corners of plate in extension. *Journal of Applied Mechanics* **19**(4), 000–000.
Numerical Recipes in FORTRAN (1992) *The Art of Scientific Computing*. 2nd edn. Cambridge University Press.
Zorin, I. S., Movchan, A. B. and Nazarov, S. A. (1988) The use of the elastic polarisation tensor in problems of crack mechanics (in Russian), *USSR Izvestiya. Mechanics of Solids* **26**(6), 128–134.

APPENDIX

In the text below we discuss two issues: existence of a solution and the numerical optimization algorithm (see Sections 2 and 3 of the main text). For more detailed analyses we refer to Sokolowski and Zolesio (1992) and Numerical Recipes in FORTRAN (1992).

Existence of the solution. To prove the existence of the solution the second constant (finite size of the cavity) is essential. Consider a closure of a bounded domain in N-dimensional space (each point of this domain specifies a set of coefficients of the conformal mapping). We exclude all unbounded domains from our consideration as they lead to failure of the second constraint.

Also we exclude the sets of coefficients which lead to self-intersection boundary. Let an N-tuple of coefficients of the conformal mapping provide the boundary with self-intersections. Then so will N-tuples in the sufficiently small neighbourhood of the original point. Thus the region in N-dimensional space describing the boundaries with self-intersection is open. Hence its complement is closed.

According to the Weierstrass theorem such a function has both maximum and minimum (taking into account the condition $\delta W < 0$ which is true for all increments associated with the cavities).

Downhill simplex method. For reader convenience we discuss below the general idea of the downhill simplex method, the optimization method, which was used in our work. For more detailed analyses we refer to Numerical Recipes in FORTRAN (1992) and the list of references mentioned there.

The downhill simplex method requires the values of the function only, and it does not require the derivatives. It simplifies the procedure; it works effectively even for the case when the function, we minimize, is not specified in the explicit analytical form. It starts not just with a single point, but with $2N+1$ points, defining an initial simplex in $2N$-dimensional space. We decide that the initial starting point $\mathbf{P}_0$ corresponds to a unit circle $\{c_n = 0\}$ and take the other points to be $\mathbf{P}_n = \mathbf{P}_0 + \lambda_n \mathbf{e}_n$, where $\mathbf{e}_n$ are $2N$ unit basis vectors and λ_n are constants representing the characteristic length scale along the direction $\mathbf{e}_n$. They are chosen by using the value $1/\sqrt{n}$ (the upper bound for the modulus of the coefficient c_n) as the characteristic length scale.

The basic idea of the downhill simplex method is to compare the values of the function at the $2N+1$ vertices of the initial simplex and move this simplex towards the minimum during the iterative process. On each step we evaluate the function at all vertices of the simplex and choose the maximal one $\mathbf{P}_m$. Then we archive the "reflection" of the point $\mathbf{P}_m$ with maximal value of the function via the simplex boundary. It means that we define a new position $\mathbf{P}_r$ of the point $\mathbf{P}_m$ in such a way that

$$\mathbf{P}_r = (1-\alpha)\mathbf{P}_* - \alpha \mathbf{P}_m,$$

where $\mathbf{P}_* = (1/2N)\sum_{n=1, n\neq m}^{2N+1} \mathbf{P}_n$ is the centroid of all points with the exception of $\mathbf{P}_m$ and α is the reflection coefficient which is the ratio of distance between $\mathbf{P}_r$ and $\mathbf{P}_*$ and the distance between $\mathbf{P}_m$ and $\mathbf{P}_*$.

The reflected point $\mathbf{P}_r$ will be on the line joining $\mathbf{P}_m$ and $\mathbf{P}_*$ on the opposite side of $\mathbf{P}_*$. Repetitive application of the reflection process leads to a step-by-step approaching in the direction of the minimum.

In the particular situation when $f(\mathbf{P}_r) > f(\mathbf{P}_n)$ for all n except $n = m$, the simplex is contracted along the direction $\mathbf{P}_r - \mathbf{P}_m$ to $\mathbf{P}_*$. Alternatively, if the reflection produces $\mathbf{P}_r$ such that $f(\mathbf{P}_r) < f(\mathbf{P}_n)$, the simplex is expanding, and we attempt to find a local minimum on the line $\mathbf{P}_r - \mathbf{P}_m$ (the one-dimensional gradient method used in this particular situation).

After application of the "expansion" or "contraction" of the simplex we go back to the reflection procedure. The following convergence criterion is used with the simplex method

$$\left(\frac{\sum_{n=1}^{2N+1} [f(P_n) - f(P_*)]^2}{2N+1} \right)^{1/2} < \varepsilon,$$

where ε is a small positive parameter. In this work we used the Numerical Recipes routine "amoeba" (Numerical Recipes in FORTRAN 1992) in realizing the downhill simplex method.